The Hamiltonian properties of supergrid graphs

Ruo-Wei Hung*, Chih-Chia Yao, and Shang-Ju Chan

Department of Computer Science and Information Engineering,
Chaoyang University of Technology,
Wufeng, Taichung 41349, Taiwan

Abstract

In this paper, we first introduce a novel class of graphs, namely supergrid. Supergrid graphs include grid graphs and triangular grid graphs as their subgraphs. The Hamiltonian cycle and path problems for grid graphs and triangular grid graphs were known to be NP-complete. However, they are unknown for supergrid graphs. The Hamiltonian cycle (path) problem on supergrid graphs can be applied to control the stitching traces of computerized sewing machines. In this paper, we will prove that the Hamiltonian cycle problem for supergrid graphs is NP-complete. It is easily derived from the Hamiltonian cycle result that the Hamiltonian path problem on supergrid graphs is also NP-complete. We then show that two subclasses of supergrid graphs, including rectangular (parallelism) and alphabet, always contain Hamiltonian cycles.

Keywords: Hamiltonian properties, supergrid graph, rectangular supergrid graph, alphabet supergrid graph, grid graph, triangular grid graph, computerized sewing machine

1. Introduction

A *Hamiltonian cycle* in a graph is a simple cycle in which each vertex of the graph appears exactly once. A *Hamiltonian path* in a graph is a simple path with the same property. The *Hamiltonian cycle* (resp., *path*) *problem* involves testing whether or not a graph contains a Hamiltonian cycle (resp., path). A graph is said to be *Hamiltonian* if it contains a Hamiltonian cycle. The *Hamiltonian problems* include Hamiltonian cycle and Hamiltonian path problems. They have numerous applications in different areas, including establishing transport routes, production launching, the on-line optimization of flexible manufacturing systems [1], computing the perceptual boundaries of dot patterns [30], pattern recognition [2, 31, 34], and DNA physical mapping [14]. It is well known that the Hamiltonian problems are NP-complete for general graphs [10, 20]. The same holds true for bipartite graphs [23], split graphs [11], circle graphs [8], undirected path graphs [3], grid graphs [19], and triangular grid graphs [12]. In this paper, we will study the Hamiltonian problems on supergrid graphs which contain grid graphs and triangular grid graphs as subgraphs.

The *two-dimensional integer grid* G^∞ is an infinite graph whose vertex set consists of all points of the Euclidean plane with integer coordinates and in which two vertices are adjacent if and only if the (Euclidean) distance between them is equal to 1. A *grid graph* is a finite, vertex-induced subgraph of G^∞. For a node v in the plane with integer coordinates, let v_x and v_y represent the x and y coordinates of node v, respectively, denoted by $v = (v_x, v_y)$. If v is a vertex in a grid graph, then its possible adjacent vertices include $(v_x, v_y - 1)$, $(v_x - 1, v_y)$, $(v_x + 1, v_y)$, and $(v_x, v_y + 1)$. For example, Fig. 1(a) depicts a fragment of graph G^∞ and Fig. 2(a) shows a grid graph. Recently, the properties of triangular grid graphs, which contain grid graphs as subgraphs, have received much attention. The *two-dimensional triangular grid* T^∞ is an infinite graph obtained from G^∞ by adding all edges on the lines traced from up-left to down-right. A *triangular grid graph* is a finite, vertex-induced subgraph of T^∞. The possible adjacent vertices of a vertex $v = (v_x, v_y)$ in a triangular grid graph contain $(v_x, v_y - 1)$, $(v_x - 1, v_y)$, $(v_x + 1, v_y)$, $(v_x, v_y + 1)$, $(v_x - 1, v_y - 1)$, and $(v_x + 1, v_y + 1)$. For instance, Fig. 1(b) depicts a fragment of graph T^∞ and Fig. 2(b) shows a triangular grid

*Corresponding author.
Email addresses: `rwhung@cyut.edu.tw` (Ruo-Wei Hung), `ccyao@cyut.edu.tw` (Chih-Chia Yao)

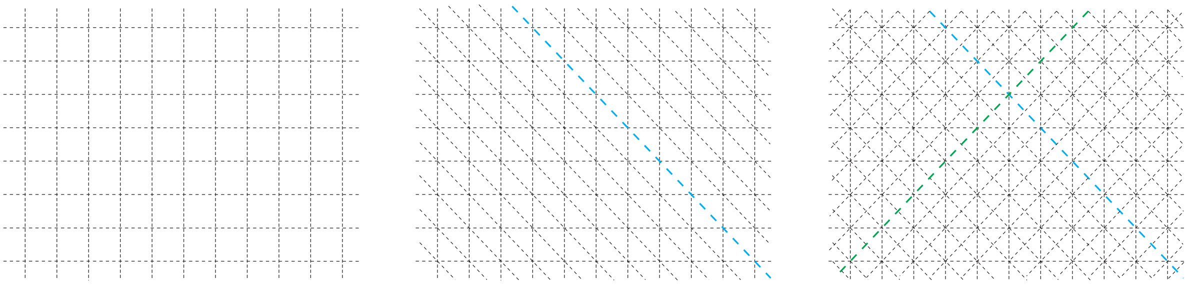

(a) (b) (c)

Fig. 1: A fragment of infinite graph (a) G^{∞}, (b) T^{∞}, and (c) S^{∞}.

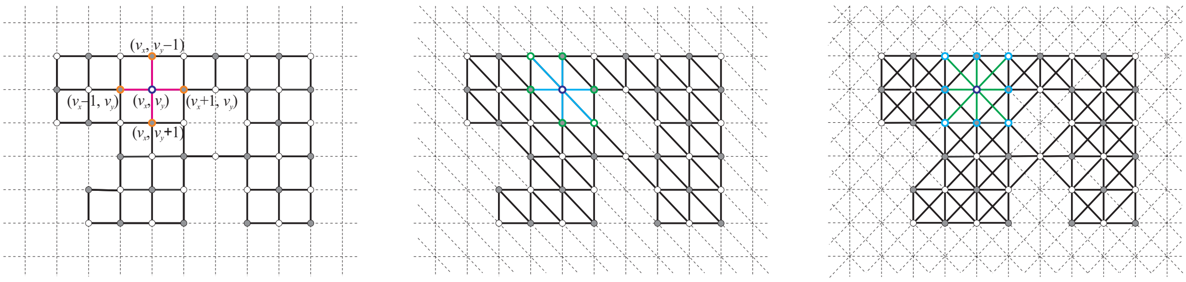

(a) (b) (c)

Fig. 2: (a) A grid graph, (b) a triangular grid graph, and (c) a supergrid graph, where solid lines indicate the edges of the graphs.

graph. Note that T^{∞} is isomorphic to the original infinite triangular grid graph in the literature [12] but these graphs are different when considered as geometric graphs. By the same construction of triangular grid graphs from grid graphs, we propose a new class of graphs, namely *supergrid graphs*, as follows. The *two-dimensional supergrid* S^{∞} is an infinite graph obtained from T^{∞} by adding all edges on the lines traced from up-right to down-left. A *supergrid graph* is a finite, vertex-induced subgraph of S^{∞}. The possible adjacent vertices of a vertex $v = (v_x, v_y)$ in a supergrid graph contain $(v_x, v_y - 1)$, $(v_x - 1, v_y)$, $(v_x + 1, v_y)$, $(v_x, v_y + 1)$, $(v_x - 1, v_y - 1)$, $(v_x + 1, v_y + 1)$, $(v_x + 1, v_y - 1)$, and $(v_x - 1, v_y + 1)$. Thus, supergrid graphs contain grid graphs and triangular grid graphs as subgraphs. For example, Fig. 1(c) depicts a fragment of graph S^{∞} and Fig. 2(c) shows a supergrid graph. Obviously, all grid graphs are bipartite [19] but triangular grid graphs and supergrid graphs are not bipartite. The Hamiltonian cycle and path problems on grid graphs and triangular grid graphs have been shown to be NP-complete [12, 19]. However, they are unknown for supergrid graphs. In this paper, we will prove that the Hamiltonian cycle and path problems for supergrid graphs are NP-complete.

The possible application for the Hamiltonian cycle (path) problem on supergrid graphs is presented as follows. Consider a computerized sewing machine given an image. The computerized sewing software is used to compute the sewing traces of a computerized sewing machine. There may be two parts in a computerized sewing software. The first part is to do image processing for the input image, e.g. reduce order of colors and image thinning. It then produces some sets of lattices in which every set of lattices represents a color in the input image for sewing. The second part is given by a set of lattices and then computes a cycle (path) to visit the lattices of the set such that each lattice is visited exactly once. Finally, the software transmits the stitching trace of the computed cycle (path) to the computerized sewing machine, and the machine then performs the sewing work along the trace on the object, e.g. clothes. For example, given an image in Fig. 3(a), the software first analyzes the image and then produces seven colors of regions in which each region is filled with the same color and may consist of some disconnected blocks, as shown in Fig. 3(b). It then produces seven sets of lattices in which every set of lattices represents a region, where each region is filled by a sewing trace with the same color and it may be partitioned into many non-contiguous blocks. Fig.

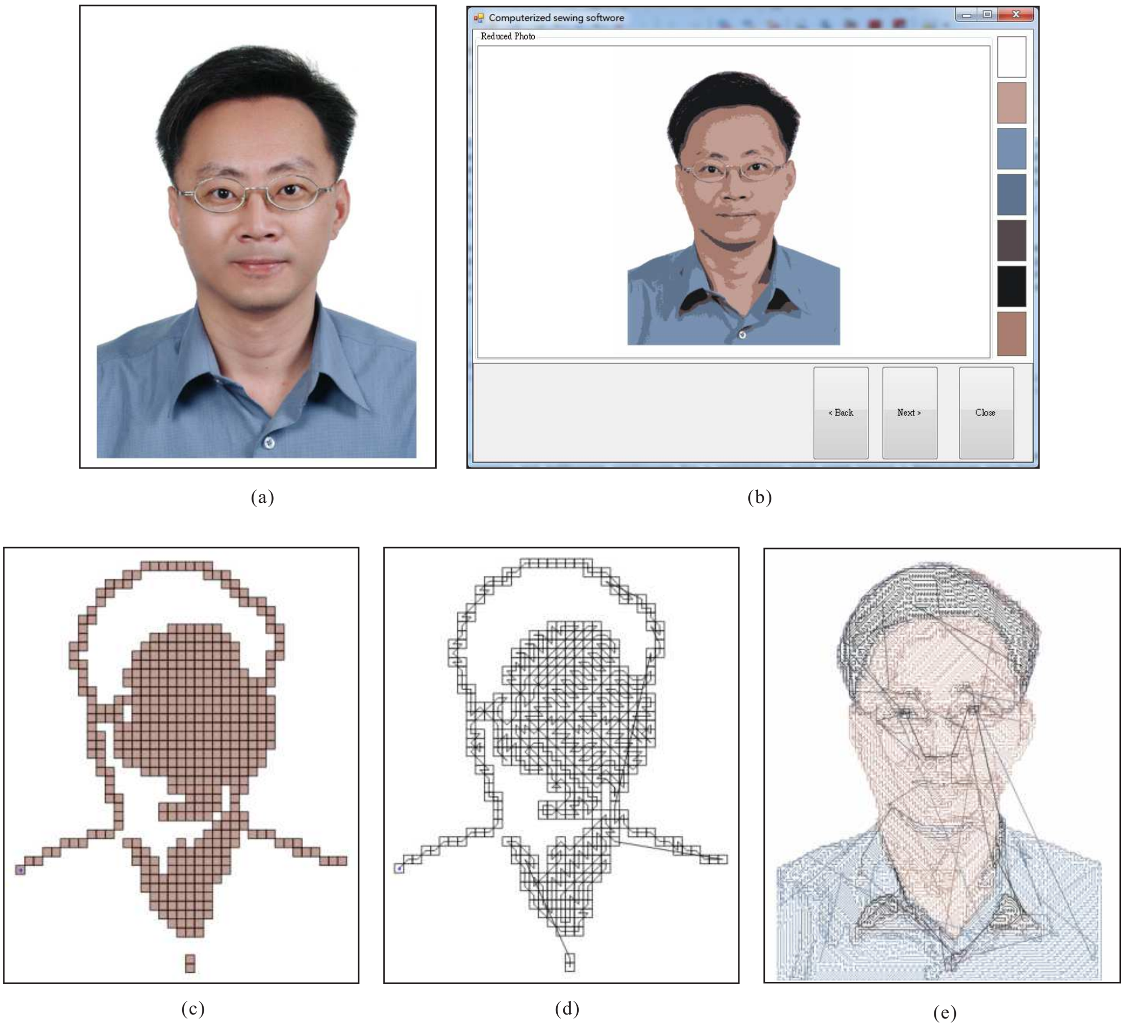

Fig. 3: (a) An input image for the computerized sewing software, (b) seven colors of regions produced by image processing, (c) a set of lattices for one region of color, (d) a possible sewing trace for the set of lattices in (c), and (e) an overview after computing sewing traces of all regions of colors.

3(c) shows a set of lattices for one region of color, and the software then computes a sewing trace for the set of lattices, as depicted in Fig. 3(d). Since each stitch position of a sewing machine can be moved to its eight neighbor positions (left, right, up, down, up-left, up-right, down-left, and down-right), one set of lattices forms a supergrid graph which may be disconnected. Note that each lattice will be represented by a vertex of a supergrid graph, each region may be separated into many blocks in which each block represented a connected supergrid graph. The desired sewing trace of each set of adjacent lattices is the Hamiltonian cycle (path) of the corresponding connected supergrid graph when it is Hamiltonian. Note that if the corresponding supergrid graph is not Hamiltonian, then the sewing trace contains more than one paths and these paths must be concatenated. After computing the sewing traces of all regions of colors, the software then transmits the computed stitching trace to the computerized sewing machine. Fig. 3(e) depicts the possible sewing result for the image in Fig. 3(a). In addition, the structure of supergrid graphs can be used to design the network topology, and its network diameter is smaller than that of grid graphs.

Related areas of investigation are summarized as follows. Itai *et al.* [19] showed that the Hamiltonian cycle and Hamiltonian path problems for grid graphs are NP-complete. They also gave the necessary and sufficient conditions for a rectangular grid graph having a Hamiltonian path between two given vertices. Zamfirescu *et al.* [35] gave the sufficient conditions for a grid graph having a Hamiltonian cycle, and proved that all grid graphs of positive width have Hamiltonian line graphs. Later, Chen *et al.* [6] improved the Hamiltonian path algorithm of [19] on rectangular grid graphs and presented a parallel algorithm for the Hamiltonian path problem with two given endpoints in rectangular grid graph (mesh). Also there is a polynomial-time algorithm for finding Hamiltonian cycles in solid grid graphs [25]. In [33], Salman introduced alphabet grid graphs and determined classes of alphabet grid graphs which contain Hamiltonian cycles. Keshavarz-Kohjerdi and Bagheri [21] gave the necessary and sufficient conditions for the existence of Hamiltonian paths in alphabet grid graphs, and presented linear-time algorithms for finding Hamiltonian paths with two given endpoints in these graphs. Recently, Keshavarz-Kohjerdi *et al.* [22] presented a linear-time algorithm for computing the longest path between two given vertices in rectangular grid graphs. The Hamiltonian cycle (path) on triangular grid graphs has been shown to be NP-complete [12]. Recently, Reay and Zamfirescu [32] proved that all 2-connected, linear-convex triangular grid graphs except one special case contain Hamiltonian cycles. They also proved that all connected, locally connected triangular grid graphs (with one exception) contain Hamiltonian cycles. In addition, the Hamiltonian cycle problem on hexagonal grid graphs was known to be NP-complete [18]. For more related works, we refer readers to [5, 7, 9, 13, 15, 16, 17, 24, 27, 28, 29, 36].

The rest of the paper is organized as follows. In Section 2, some notations and basic terminologies are introduced. Section 3 shows that the Hamiltonian cycle and Hamiltonian path problems for supergrid graphs are NP-complete. In Section 4, we show that rectangular (parallelism) and alphabet supergrid graphs are Hamiltonian. Finally, we make some concluding remarks in Section 5.

2. Notations and terminologies

In this section, we will introduce fundamental terminologies and symbols used in the paper. For graph-theoretic terminology not defined in this paper, the reader is referred to [4]. Let $G = (V, E)$ be a graph with vertex set $V(G)$ and edge set $E(G)$. Let S be a subset of vertices in G, and let u, v be two vertices in G. We write $G[S]$ for the subgraph of G *induced* by S, $G - S$ for the subgraph $G[V - S]$, i.e., the subgraph induced by $V - S$. In general, we write $G - v$ instead of $G - \{v\}$. If (u, v) is an edge in G, we say that u is *adjacent* to v and u, v are *incident* to edge (u, v). The notation $u \sim v$ (resp., $u \nsim v$) means that vertices u and v are adjacent (resp., non-adjacent). A *neighbor* of v in G is any vertex that is adjacent to v. We use $N_G(v)$ to denote the set of neighbors of v in G. The subscript 'G' of $N_G(v)$ can be removed from the notation if it has no ambiguity. The *degree* of vertex v is the number of vertices adjacent to the vertex v. The *distance* between u and v is the length of the shortest path between these two vertices. A path P of length $|P| - 1$ in a graph G, denoted by $v_1 \rightarrow v_2 \rightarrow \cdots \rightarrow v_{|P|-1} \rightarrow v_{|P|}$, is a sequence $(v_1, v_2, \cdots, v_{|P|-1}, v_{|P|})$ of vertices such that $(v_i, v_{i+1}) \in E(G)$ for $1 \leqslant i < |P|$. The first and last vertices visited by path P are denoted by $start(P)$ and $end(P)$, respectively. We will use $v_i \in P$ to denote "P visits vertex v_i" and use $(v_i, v_{i+1}) \in P$ to denote "P visits edge (v_i, v_{i+1})". A path from vertex v_1 to vertex v_k is denoted by (v_1, v_k)-path. In addition, we use P to refer to the set of vertices visited by path P if it is understood without ambiguity. On the other hand, a path is called the *reversed path*, denoted by rev(P), of path P if it visits the vertices of P from $end(P)$ to $start(P)$ in proper sequence; that is, the reversed path rev(P) of $P = v_1 \rightarrow v_2 \rightarrow \cdots \rightarrow v_{|P|-1} \rightarrow v_{|P|}$ is $v_{|P|} \rightarrow v_{|P|-1} \rightarrow \cdots \rightarrow v_2 \rightarrow v_1$. A cycle is a path C such that $|V(C)| \geqslant 3$ and $start(C) \sim end(C)$.

Let S^∞ be the infinite graph whose vertex set consists of all points of the plane with integer coordinates and in which two vertices are adjacent if and only if the difference of their x or y coordinates is not larger than 1. A *supergrid graph* is a finite, vertex-induced subgraph of S^∞. For a vertex v in a supergrid graph, let v_x and v_y denote respectively x and y coordinates of its corresponding point. We color vertex v to be *white* if $v_x + v_y \equiv 0 \pmod 2$; otherwise, v is colored to be *black*. Then there are eight possible neighbors of vertex v including four white vertices and four black vertices. Obviously, all grid graphs are bipartite [19] but supergrid graphs are not bipartite.

Rectangular grid graphs first appeared in [26], where Luccio and Mugnia tried to solve the Hamiltonian path problem on them. Itai *et al.* [19] gave necessary and sufficient conditions for the existence of Hamiltonian (s, t)-path in rectangular grid graphs, where s, t are two given vertices. In this paper, we expand them to a subclass of supergrid graphs, namely rectangular supergrid graphs. Let $R(m, n)$ be the supergrid graph whose vertex set $V(R(m, n)) = \{v = (v_x, v_y) \mid 1 \leqslant v_x \leqslant m \text{ and } 1 \leqslant v_y \leqslant n\}$. Then, $R(m, n)$ contains m columns and n rows of vertices in S^∞. A *rectangular supergrid graph* is a supergrid graph that is isomorphic to $R(m, n)$ for $m, n \geqslant 1$. Thus m and n, the *dimensions*, specify a rectangular supergrid graph up to isomorphism. The size of $R(m, n)$ is defined to be mn, and $R(m, n)$ is called n-rectangle. The edge in the boundary of $R(m, n)$ is called *boundary edge*. For example, Fig. 4(a)

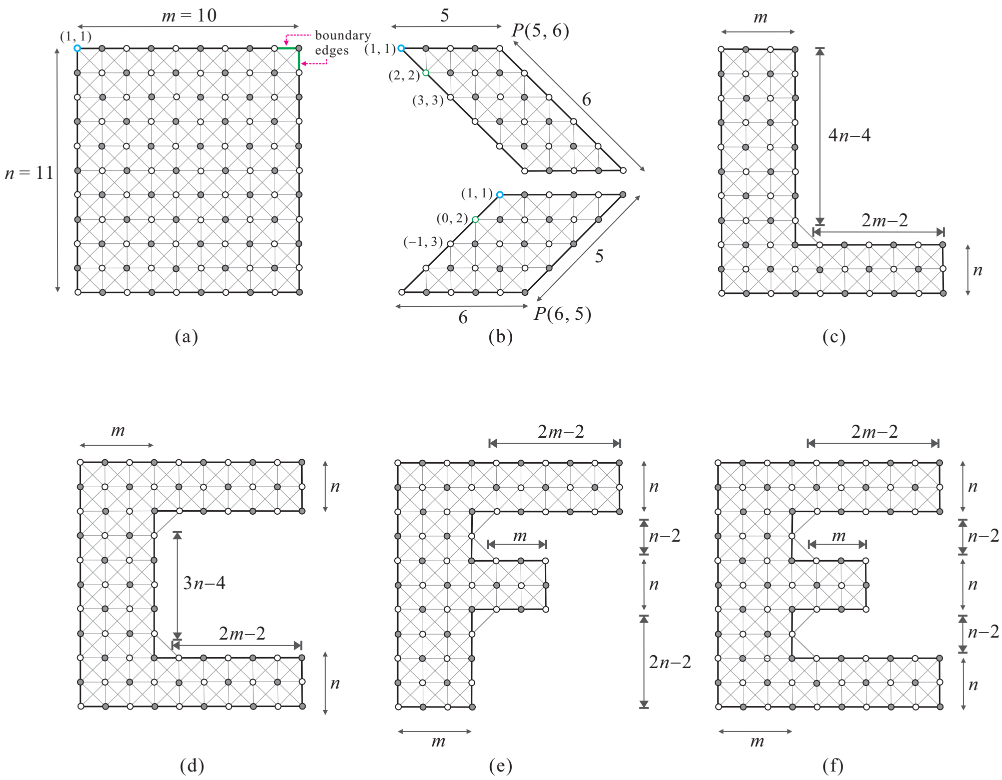

Fig. 4: Rectangular, parallelism, and alphabet supergrid graphs, where (a) a rectangular supergrid graph $R(10, 11)$, (b) two parallelism supergrid graphs $P(5, 6)$ and $P(6, 5)$, (c) an L-alphabet supergrid graph $L(4, 3)$, (d) an C-alphabet supergrid graph $C(4, 3)$, (e) an F-alphabet supergrid graph $F(4, 3)$, and (f) an E-alphabet supergrid graph $E(4, 3)$.

shows a rectangular supergrid graph $R(10, 11)$ which is called 11-rectangle and contains $2(9 + 10) = 38$ boundary edges. In the figures, we assume that $(1, 1)$ is the coordinates of the up-left vertex, i.e. the leftmost vertex of the first row, in a supergrid graph. A *parallelism* supergrid graph is defined similar to $R(m, n)$. Let $P(m, n)$ be the supergrid graph with $m \geqslant n$ whose vertex set $V(P(m, n)) = \{v = (v_x, v_y) \mid 1 \leqslant v_y \leqslant n$ and $v_y \leqslant v_x \leqslant v_y + m - 1\}$ or $\{v = (v_x, v_y) \mid 1 \leqslant v_y \leqslant n$ and $2 - v_y \leqslant v_x \leqslant m - v_y + 1\}$. A *parallelism supergrid graph* is a supergrid graph which is isomorphic to $P(m, n)$. For example, Fig. 4(b) depicts two parallelism supergrid graphs $P(5, 6)$ and $P(6, 5)$. In the above definition, there are two types of parallelism supergrid graphs. We can see that they are isomorphic although they are different when considered as geometric graphs. Note that the boundary edges of $R(m, n)$ and $P(m, n)$ form a rectangle and a parallelogram, respectively.

In [33], Salman first introduced alphabet grid graphs, which form a subclass of grid graphs, and studied some properties of these graphs. Recently, Keshavarz-Kohjerdi and Bagheri [21] determined the necessary and sufficient conditions for the existence of Hamiltonian (s, t)-path in alphabet grid graphs, where s, t are two given vertices. In this paper, we extend them to form a subclass of supergrid graphs, namely alphabet supergrid graphs. An *alphabet supergrid graph* is a finite vertex-induced subgraph of the rectangular supergrid graph of a certain type, as follows. For $m, n \geqslant 3$, an L-alphabet supergrid graph $L(m, n)$, C-alphabet supergrid graph $C(m, n)$, F-alphabet supergrid graph $F(m, n)$, and E-alphabet supergrid graph $E(m, n)$ are subgraphs of $R(3m - 2, 5n - 4)$. These alphabet supergrid graphs are defined as shown in Fig. 4(c) – (f), where $m = 4$ and $n = 3$.

3. NP-completeness

In this section, we will prove that the Hamiltonian cycle (path) problem for supergrid graphs is NP-complete. In [19] and [12], the authors showed the Hamiltonian cycle problem for grid graphs and triangular grid graphs to be

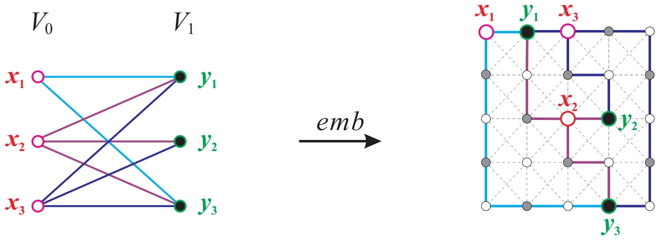

(a) (b)

Fig. 5: (a) A planar bipartite graph B with maximum degree 3, and (b) a parity-preserving embedding $emb(B)$ of B, where solid lines indicate the edges in the embedding paths.

NP-complete. We apply the idea of these proofs to show that the Hamiltonian cycle problem remains NP-complete for supergrid graphs. By using similar arguments, we can prove that the Hamiltonian path problem on supergrid graphs is still NP-complete. Notice that grid graphs and triangular grid graphs are not subclasses of supergrid graphs; these classes of graphs have common elements (vertices) but in general they are distinct.

To prove the Hamiltonian cycle problem on supergrid graphs to be NP-complete, we establish a polynomial-time reduction from the Hamiltonian cycle problem for planar bipartite graphs with maximum degree 3. The following theorem was given in [19].

Theorem 3.1. *(See [19].) The Hamiltonian cycle problem for planar bipartite graphs with maximum degree 3 is NP-complete.*

Let $B = (V_0 \cup V_1, E)$ be a planar bipartite graph with maximum degree 3 and let G_1 be a rectangular supergrid graph, where V_0 and V_1 are the bipartition sets of B in which every edge joins a vertex in V_0 and a vertex in V_1. Similarly to the parity-preserving embedding [19] of a bipartite graph into a rectangular grid graph, let us introduce the following parity-preserving embedding *emb* of B into G_1 (a one-to-one function from $V_0 \cup V_1$ to the vertices of G_1 and from E to paths in G_1):
1. The vertices of V_0 are mapped to white vertices of G_1, i.e., if $v \in V_0$, then $emb(v)$ is colored by white.
2. The vertices of V_1 are mapped to black vertices of G_1, i.e., if $v \in V_1$, then $emb(v)$ is colored by black.
3. The edges of B are mapped to vertex-disjoint paths of G_1, i.e., if $e = (u, v) \in E$, then $emb(e)$ is a path P from $emb(u)$ to $emb(v)$, and the intermediate vertices of P do not belong to any other path.

For example, Fig. 5(a) shows a planar bipartite graph B with maximum degree 3, and a parity-preserving embedding $emb(B)$ of B is depicted in Fig. 5(b). The following lemma is given in [19] and shows that the above parity-preserving embedding can be done in polynomial time.

Lemma 3.2. *(See [19].) Let B be a planar bipartite graph with n vertices and maximum degree 3. Then, a parity-preserving embedding $emb(B)$ of B into a rectangular grid (supergrid) graph $R(kn, kn)$ can be done in polynomial time, where k is a constant.*

Now given a planar bipartite graph B with n vertices and maximum degree 3, we shall construct a supergrid graph G_s such that B has a Hamiltonian cycle if and only if G_s contains a Hamiltonian cycle. Let $B = (V_0 \cup V_1, E)$. The construction of G_s from B is sketched as follows. First, we embed graph B into a rectangular supergrid graph $R(kn, kn)$ for some constant k, as described in Lemma 3.2. Let the embedding supergrid graph be G_1. In the second step, we enlarge the supergrid graph G_1 such that each edge in G_1 is transformed into a path with 9 edges. Let the enlarged supergrid graph be G_2. For example, Fig. 6 shows the supergrid graph G_2 enlarged from the supergrid graph G_1 in Fig. 5(b) for the planar bipartite graph B in Fig. 5(a). In the third step, each vertex of graph B is transformed into a *cluster* which is a small supergrid graph. The vertex of B is called *critical vertex* in G_2. Finally, each path in G_2 is simulated by a *tentacle* which is a series of 2-rectangles, and the resultant graph is a supergrid graph G_s.

Now, we introduce clusters and tentacles as follows. We transform each vertex of V_0 into a *white cluster* and each vertex of V_1 into a *black cluster*. A white cluster is a supergrid graph with 17 vertices and a black cluster is also a supergrid graph with 13 vertices. Fig. 7 shows the white and black clusters. The center of a white cluster (resp., black

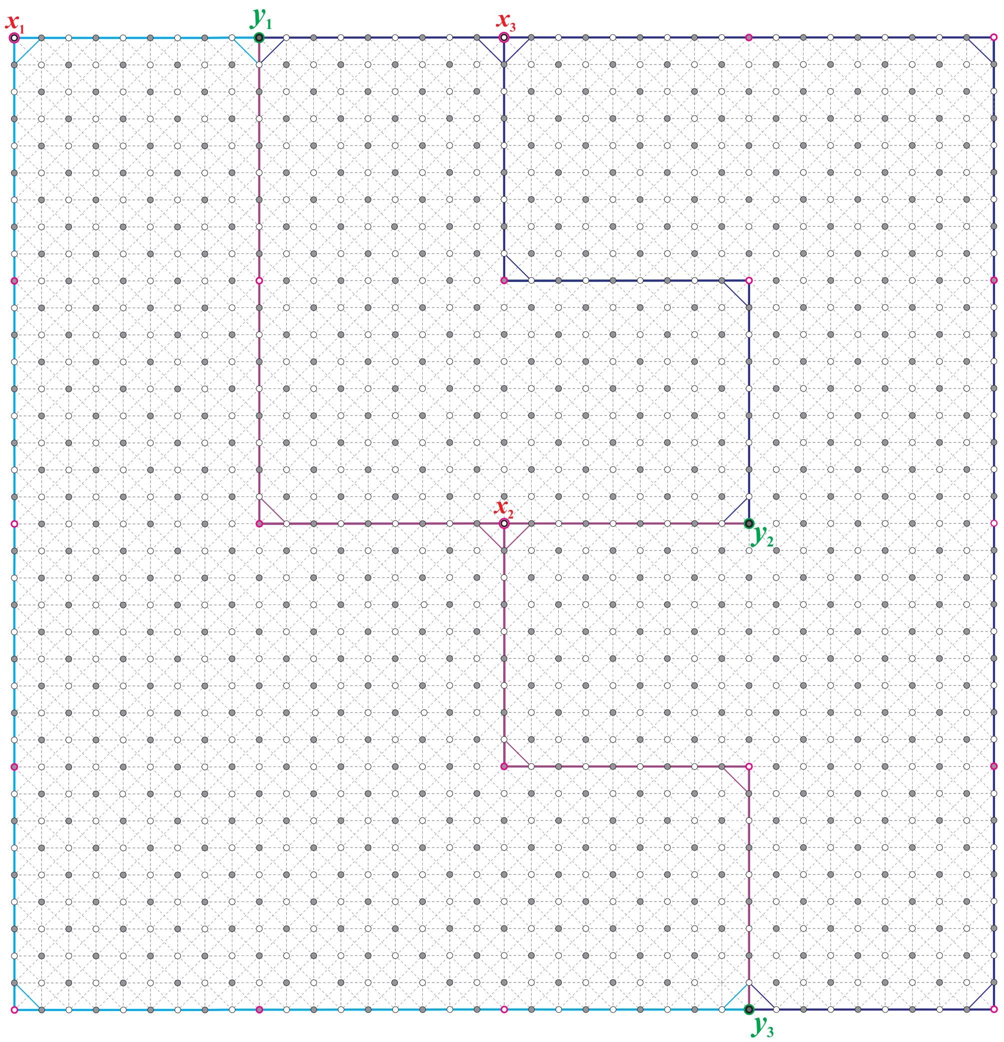

Fig. 6: The enlarged supergrid graph G_2 from the embedding supergrid graph G_1 in Fig. 5(b), where solid lines indicate the edges in G_2.

cluster) is a white critical vertex (resp., black critical vertex). For example, critical vertex x (resp., y) is the center of a white cluster (resp., a black cluster) in Fig. 7(a) (resp., Fig. 7(b)). The distance between any vertex and center in a cluster is at most 2. The vertices a_1, a_2, a_3, a_4 (resp., b_1, b_2, b_3, b_4) in Fig. 7(a) (resp., Fig. 7(b)) are called the *corner vertices* of cluster, and the edges e_1, e_2, e_3, e_4 in Fig. 7 are called *critical edges*. In our construction, the corner vertices together with critical edges of a cluster are used to connect to the other cluster. The following two propositions show the properties of clusters.

Proposition 3.3. *Let C_{17} be a white cluster, a_1, a_2, a_3, a_4 be its corner vertices, and let e_1, e_2, e_3, e_4 be its critical edges, as in Fig. 7(a). Then for $1 \leqslant i < j \leqslant 4$, there exists a Hamiltonian (a_i, a_j)-path of C_{17} which contains all four critical edges $\{e_1, e_2, e_3, e_4\}$.*

Proof. By inspection, the lemma can be verified. For example, Fig. 8(a) and Fig. 8(b) depict a Hamiltonian (a_1, a_3)-path and a Hamiltonian (a_1, a_4)-path of C_{17}, respectively, which contain all critical edges $\{e_1, e_2, e_3, e_4\}$. □

Proposition 3.4. *Let C_{13} be a black cluster, b_1, b_2, b_3, b_4 be its corner vertices, and let e_1, e_2, e_3, e_4 be its critical edges, as in Fig. 7(b). Then for $1 \leqslant i < j \leqslant 4$, there exists a Hamiltonian (b_i, b_j)-path of C_{13} which contains all four critical edges $\{e_1, e_2, e_3, e_4\}$.*

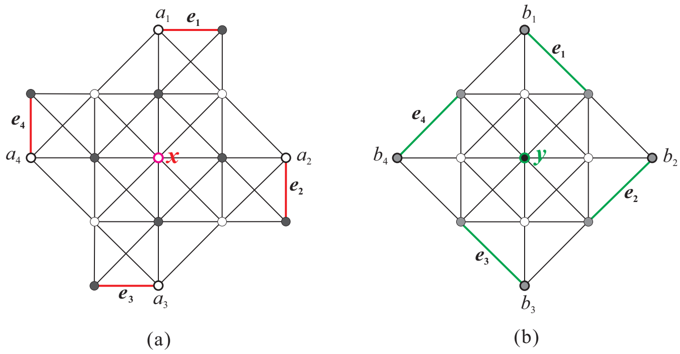

Fig. 7: (a) A white cluster C_{17}, and (b) a black cluster C_{13}, where the centers of C_{17} and C_{13} are critical vertices x and y, respectively, the critical edges include e_1, e_2, e_3, e_4, and the corner vertices include a_1, a_2, a_3, a_4 or b_1, b_2, b_3, b_4.

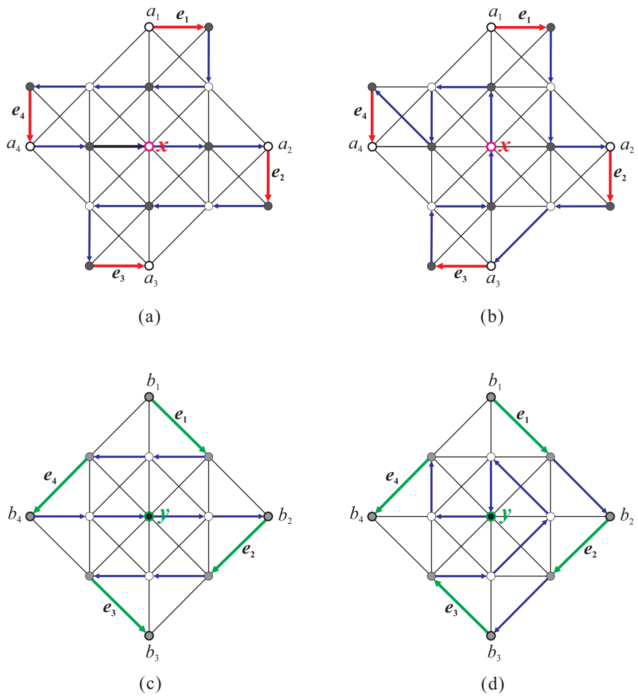

Fig. 8: (a) A Hamiltonian (a_1, a_3)-path of a white cluster C_{17}, (b) a Hamiltonian (a_1, a_4)-path of a white cluster, (c) a Hamiltonian (b_1, b_3)-path of a black cluster C_{13}, and (d) a Hamiltonian (b_1, b_4)-path of a black cluster, where arrow lines indicate the edges in such a path and each critical edge is contained in the Hamiltonian path.

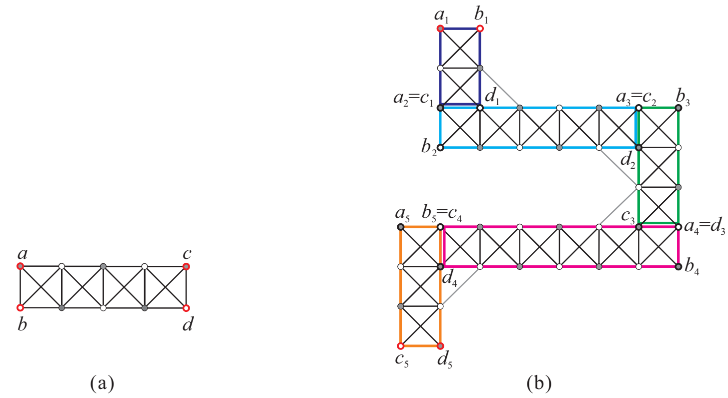

Fig. 9: (a) A strip $S(a, b; c, d)$ with corners a, b, c, d, and (b) a square tentacle $T'(a_1, b_1; c_5, d_5)$ consisting of 5 strips.

Proof. By inspection. For example, For example, Fig. 8(c) and Fig. 8(d) depict a Hamiltonian (b_1, b_3)-path and a Hamiltonian (b_1, b_4)-path of C_{13}, respectively, which contain all critical edges $\{e_1, e_2, e_3, e_4\}$. □

In our construction, the path in G_2 is simulated by a series of 2-rectangles, called *tentacle*. We will use the similar technique in [19] to make it. A *strip* is a rectangular supergrid graph with at least 2 squares (see Fig. 9(a)), i.e., it is isomorphic to $R(m, 2)$ with $m \geqslant 3$. The strip with corners a, b, c, d (the degree of every corner is 3), as in Fig. 9(a), is denoted by $S(a, b; c, d)$. A square in a strip is called *terminal* if it contains corners. A *square tentacle* T' is a supergrid graph which is either a strip or a union of a series of strips stuck together by the edges of terminal squares. Let $T' = S(a_1, b_1; c_1, d_1) \cup S(a_2, b_2; c_2, d_2) \cup \cdots \cup S(a_k, b_k; c_k, d_k)$. We define T' to satisfy the following conditions:
(1) both $c_i, d_i \in V(S(a_{i+1}, b_{i+1}; c_{i+1}, d_{i+1}))$ for $1 \leqslant i \leqslant k-1$,
(2) one of $a_{i+1}, b_{i+1} \in V(S(a_i, b_i; c_i, d_i))$ for $1 \leqslant i \leqslant k-1$, and
(3) there is no other intersection between the vertex sets of the strips.
The vertices a_1, b_1, c_k, d_k are called the corners of T', and denote this square tentacle by $T'(a_1, b_1; c_k, d_k)$. For example, Fig. 9(b) shows a square tentacle with 5 strips and corners a_1, b_1, c_5, d_5.

In the construction of an enlarged supergrid graph G_2 (see Fig. 6) from a planar bipartite graph B (see Fig. 5(a)), the path in G_2 is a combination of four possible types of subpaths, as shown in Fig. 10(a). The corresponding square tentacles for these types of subpaths are depicted in Fig. 10(b). A *tentacle* is then constructed from a square tentacle by attaching a triangle to its terminal square. For instance, Fig. 10(c) depicts the possible tentacles for the square tentacle of type I in Fig. 10(b). We call the attached triangle of a tentacle to be the *tail* of the tentacle. Let u, v be two vertices of the first square in a tentacle T such that their degrees are 3, and let w be a vertex of the tail in a tentacle T such that its degree 2. Since each strip of a tentacle is isomorphic to a 2-rectangle $R(m, 2)$ with $m \geqslant 3$, the vertices u, v exist. Then we denote the tentacle by $T(u, v; w)$. The vertices u, v are called the *twin corners* of $T(u, v; w)$, and the vertex w is said to be the *tail corner* of $T(u, v; w)$. Fig.10(c) also depicts the corners of tentacles. The following lemma shows the Hamiltonian property of a tentacle.

Lemma 3.5. *Let $T(u, v; w)$ be a tentacle. Then for any two corners $s, t \in \{u, v, w\}$, there exists a Hamiltonian (s, t)-path of $T(u, v; w)$.*

Proof. Let $T'(a_1, b_1; c_\eta, d_\eta) = S(a_1, b_1; c_1, d_1) \cup S(a_2, b_2; c_2, d_2) \cup \cdots \cup S(a_\eta, b_\eta; c_\eta, d_\eta)$ be the corresponding square tentacle of $T(u, v; w)$. That is, $T(u, v; w)$ is constructed from $T'(a_1, b_1; c_\eta, d_\eta)$ by attaching a triangle with vertices c_η, d_η, w. Then, $u, v \in \{a_1, b_1\}$ and w is adjacent to both of c_η and d_η. We claim that $T'(a_1, b_1; c_\eta, d_\eta)$ contains a Hamiltonian (s', t')-path for $s', t' \in \{a_1, b_1\}$ such that edge (c_η, d_η) is in the Hamiltonian path, and has a Hamiltonian (s', t')-path for $s' \in \{a_1, b_1\}$ and $t' \in \{c_\eta, d_\eta\}$. Since $u, v \in \{a_1, b_1\}$ and w is adjacent to both of c_η and d_η, the lemma hence holds true.

We prove the above claim by induction on η, the number of strips in square tentacle $T'(a_1, b_1; c_\eta, d_\eta)$. Initially, let $\eta = 1$. Then, $T'(a_1, b_1; c_1, d_1) = S(a_1, b_1; c_1, d_1)$. By inspection, it is easy to verify that there exists a Hamiltonian (a_1, b_1)-path of strip $S(a_1, b_1; c_1, d_1)$ such that edge (c_1, d_1) is in it. That is, the Hamiltonian path contains

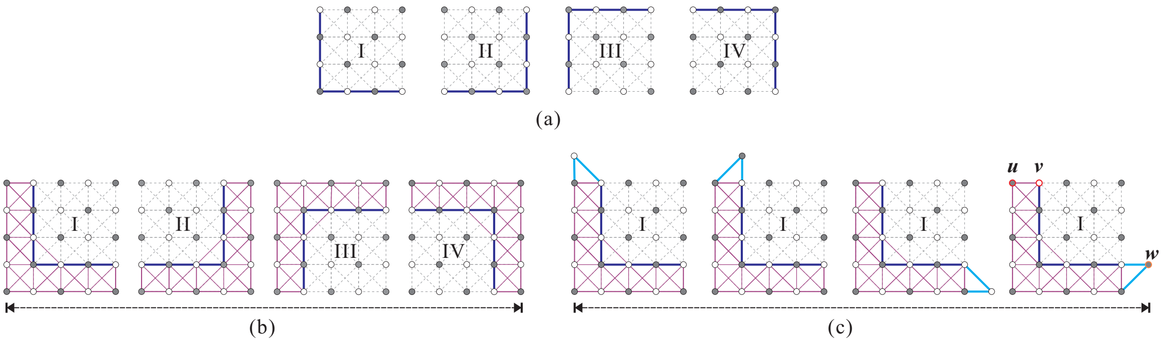

Fig. 10: (a) The possible types of subpaths in an enlarged supergrid graph G_2, (b) the corresponding square tentacles for these subpaths in (a), and (c) the possible tentacles for the square tentacle of type I in (b), where the solid lines indicate the edges in paths.

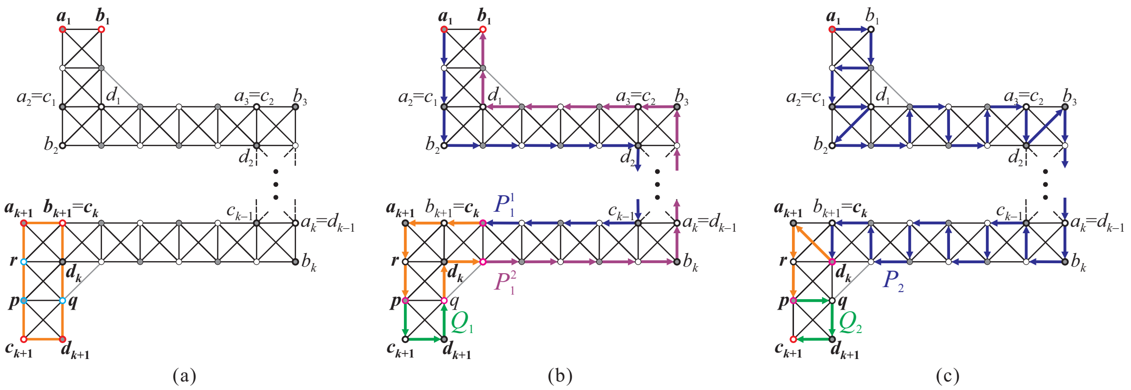

Fig. 11: (a) A schematic diagram for the relative location of $a_{k+1}, b_{k+1}, d_k, r, p, q, c_{k+1}, d_{k+1}$, (b) the Hamiltonian (a_1, b_1)-path of $T'(a_1, b_1; c_{k+1}, d_{k+1})$, and (c) the Hamiltonian (a_1, c_{k+1})-path of $T'(a_1, b_1; c_{k+1}, d_{k+1})$, where arrow lines indicate the edges in the Hamiltonian paths.

its all boundary edges except edge (a_1, b_1). In addition, for $s' \in \{a_1, b_1\}$ and $t' \in \{c_1, d_1\}$ we can easily construct a Hamiltonian (s', t')-path of $S(a_1, b_1; c_1, d_1)$. Now, assume that the claim holds true when $\eta = k \geqslant 1$. Then, there exists a Hamiltonian (a_1, b_1)-path P_1 of $T'(a_1, b_1; c_k, d_k)$ such that edge (c_k, d_k) is in P_1, and there exists a Hamiltonian (s', t')-path P_2 of $T'(a_1, b_1; c_k, d_k)$ for $s' \in \{a_1, b_1\}$ and $t' \in \{c_k, d_k\}$. Consider that $\eta = k + 1$. Then, $T'(a_1, b_1; c_{k+1}, d_{k+1}) = T'(a_1, b_1; c_k, d_k) \cup S(a_{k+1}, b_{k+1}; c_{k+1}, d_{k+1})$. By definition of square tentacle, one of $a_{k+1}, b_{k+1} \in \{c_k, d_k\}$ and both $c_k, d_k \in V(S(a_{k+1}, b_{k+1}; c_{k+1}, d_{k+1}))$. Without loss of generality, suppose that $b_{k+1} = c_k$ and the first square of $S(a_{k+1}, b_{k+1}; c_{k+1}, d_{k+1})$ contains vertices $a_{k+1}, b_{k+1} = c_k, d_k, r$. Let $S' = S(p, q; c_\tau, d_\tau)$ be a strip obtained from $S(a_{k+1}, b_{k+1}; c_{k+1}, d_{k+1})$ by removing the vertices of the first square. Since each strip contains at least two squares, we have that $S' \neq \emptyset$, $c_\tau = c_{k+1}$, and $d_\tau = d_{k+1}$. Note that if $S(a_{k+1}, b_{k+1}; c_{k+1}, d_{k+1})$ contains only two squares, then $p = c_{k+1}$ and $q = d_{k+1}$. The relative location of $a_{k+1}, b_{k+1}, d_k, r, p, q, c_{k+1}, d_{k+1}$ is depicted in Fig. 11(a). Then, d_k, r, p, q forms the second square of $S(a_{k+1}, b_{k+1}; c_{k+1}, d_{k+1})$. Note that each square of a strip is a clique. Consider the following two cases:

Case 1: $s', t' \in \{a_1, b_1\}$. By the induction hypothesis, there exists a Hamiltonian (a_1, b_1)-path P_1 of $T'(a_1, b_1; c_k, d_k)$ such that edge (c_k, d_k) is in P_1. Without loss of generality, suppose that $P_1 = P_1^1 \to c_k \to d_k \to P_1^2$, i.e., c_k appears before d_k in P_1, where $start(P_1^1), end(P_1^2) \in \{a_1, b_1\}$. The case that c_k appears after d_k in P_1 can be verified similarly. By inspection, we can construct a Hamiltonian (p, q)-path Q_1 of $S' = S(p, q; c_{k+1}, d_{k+1})$ such that edge $(c_{k+1}, d_{k+1}) \in Q_1$. Let $P^* = P_1^1 \to c_k \to a_{k+1} \to r \to Q_1 \to d_k \to P_1^2$. Then, P^* is a Hamiltonian (a_1, b_1)-path of $T'(a_1, b_1; c_{k+1}, d_{k+1})$ such that edge (c_{k+1}, d_{k+1}) is in P^*. The construction of such a Hamiltonian (a_1, b_1)-path P^* is depicted in Fig. 11(b).

Case 2: $s' \in \{a_1, b_1\}$ and $t' \in \{c_{k+1}, d_{k+1}\}$. By the induction hypothesis, there exists a Hamiltonian (s', d_k)-path P_2

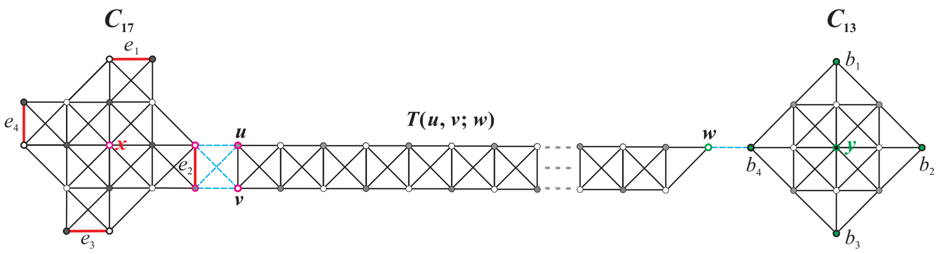

Fig. 12: The connection of two clusters via a tentacle, where dashed lines represent the edges between cluster and tentacle.

of $T'(a_1, b_1; c_k, d_k)$. By inspection, we can construct a Hamiltonian (p, t')-path Q_2 of $S' = S(p, q; c_{k+1}, d_{k+1})$, where $t' \in \{c_{k+1}, d_{k+1}\}$. Let $P' = P_2 \rightarrow a_{k+1} \rightarrow r \rightarrow Q_2$. Then, P' is a Hamiltonian (s', t')-path of $T'(a_1, b_1; c_{k+1}, d_{k+1})$, where $s' \in \{a_1, b_1\}$ and $t' \in \{c_{k+1}, d_{k+1}\}$. The construction of such a Hamiltonian (a_1, c_{k+1})-path P' is shown in Fig. 11(c).

It immediately follows from the above cases that the claim holds true. This completes the proof of the lemma. □

Let $B = (V_0 \cup V_1, E)$ be a planar bipartite graph with n vertices and maximum degree 3, G_1 be the embedding supergrid graph from B, and let G_2 be the enlarged supergrid graph by multiplying the scale of G_1 by 9. We have simulated the critical vertices of G_2 by clusters and the paths of G_2 by tentacles. The remaining care is taken as to how the tentacle is connected to the clusters corresponding to two critical vertices of G_2. Let $x \in V_0$ and $y \in V_1$ with $(x, y) \in E(B)$. Then, we simulate x and y by a white cluster C_{17} and a black cluster C_{13}, respectively, such that C_{17} contains the white vertex x as center and four critical edges e_1, e_2, e_3, e_4, and C_{13} contains the black vertex x as center and four corner vertices b_1, b_2, b_3, b_4, as shown in Fig. 7. The path between x and y in G_2 is then simulated by a tentacle $T(u, v; w)$. Tentacle $T(u, v; w)$ is used to connect clusters C_{17} and C_{13} in the following way. The twin corners, u and v, of $T(u, v; w)$ are adjacent to the vertices of one critical edge in C_{17}, and the other corner, w, of $T(u, v; w)$ is adjacent to one corner vertex of C_{13}. For example, Fig. 12 depicts such a connection between white cluster C_{17} and black cluster C_{13} via a tentacle $T(u, v; w)$. Since the maximum degree of the original planar bipartite graph is 3, the number of tentacles connecting to each cluster is at most 3. For a white cluster (resp., black cluster), there are four critical edges (resp., corner vertices) (see Fig. 7) and the number of critical edges (resp., corner vertices) used to connect tentacles is at most 3 since the maximum degree of the original planar bipartite graph is 3. Thus, it is enough to make such a connection. On the other hand, the paths in embedding supergrid graph G_1 are vertex disjoint and hence they are vertex disjoint paths in the enlarged supergrid graph G_2. Since we enlarge the scale of G_1 by 9, i.e., each edge in G_1 is transformed into a path with 9 edges, it is easy to construct tentacles from the paths of G_2 such that tentacles are disjoint.

Let $T(u, v; w)$ be a tentacle with twin corners u, v and tail corner w. By Lemma 3.5, there exists a Hamiltonian (s, t)-path of $T(u, v; w)$ for $s, t \in \{u, v, w\}$. By the definition of tentacle, u, v are adjacent and w is adjacent to neither u nor v. We can easily observe that there are only two types of Hamiltonian (s, t)-paths in $T(u, v; w)$. The path can be either a *return* path if s, t are twin corners or a *cross* path if one of s, t is tail corner. For example, Fig. 13 depicts these two types of Hamiltonian paths in $T(u, v; w)$ shown in Fig. 12. Note that there are many return paths and cross paths.

We have introduced how to construct a supergrid graph G_s from a planar bipartite graph B with maximum degree 3. The construction algorithm is formally presented as follows.

Algorithm SupergridConstruction
Input: $B = (V_0 \cup V_1, E)$, a planar bipartite graph with maximum degree 3.
Output: G_s, a supergrid graph constructed from B.
Method:

1. embed graph B into a rectangular supergrid graph $R(kn, kn)$ for some constant k [19], and let the embedding supergrid graph be G_1;
2. enlarge G_1 to a supergrid graph G_2 such that each edge in G_1 is transformed into a path with 9 edges;
3. **for** each white critical vertex x of G_2 ($x \in V_0$), x is transformed into a white cluster C_{17} with center x;
4. **for** each black critical vertex y of G_2 ($y \in V_1$), y is transformed into a black cluster C_{13} with center y;

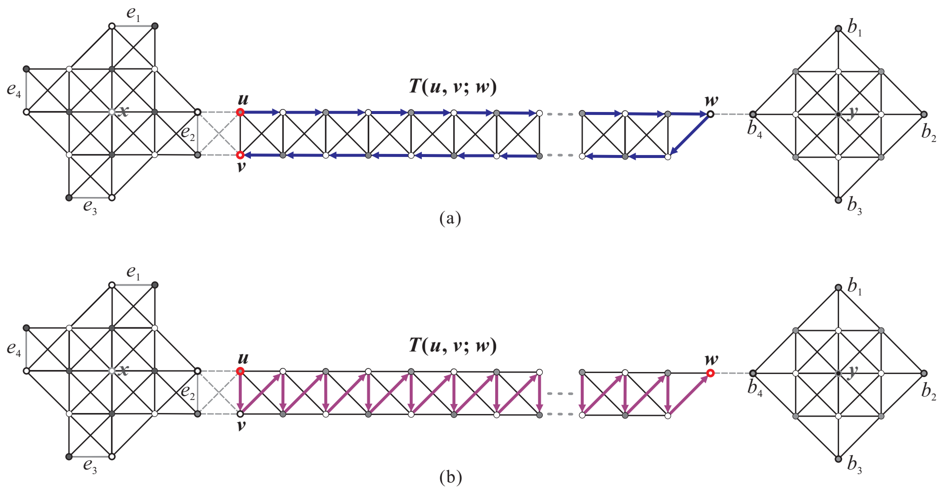

Fig. 13: (a) A return path, and (b) a cross path in a tentacle $T(u, v; w)$ shown in Fig. 12, where arrow lines indicate the paths.

5. **for** each path between white critical vertex x and black critical vertex y, construct a tentacle $T(u, v; w)$ to connect the corresponding clusters of x and y such that u, v are adjacent to two vertices of one critical edges in white cluster and w is adjacent to one corner vertex of black cluster;
6. let the constructed supergrid graph be G_s and **output** G_s.

For example, given a planar bipartite graph $B = (V_0 \cup V_1, E)$ with maximum degree 3 shown in Fig. 5(a), the embedding supergrid graph G_1 is shown in Fig. 5(b). The enlarged supergrid graph G_2 by multiplying the scale of G_1 by 9 is shown in Fig. 6. The constructed supergrid graph G_s is depicted in Fig. 14. By Lemma 3.2, line 1 of Algorithm SupergridConstruction can be done in polynomial time. Clearly, lines 2–6 of the algorithm can be done in polynomial time. Then, Algorithm SupergridConstruction runs in polynomial time and hence the following lemma holds true.

Lemma 3.6. *Given a planar bipartite graph $B = (V_0 \cup V_1, E)$ with maximum degree 3, Algorithm SupergridConstruction constructs a supergrid graph G_s in polynomial time.*

Next, we will prove that supergrid graph G_s has a Hamiltonian cycle if and only if there exists a Hamiltonian cycle in the planar bipartite graph B. Before proving the above property, we first give the relation between tentacle and Hamiltonian cycle of G_s. For a cycle C of a graph G and a subgraph H of G, we denote the restriction of C to H by $C_{|H}$. Then, $C_{|H}$ is a set of subpaths of C. We then have the following lemma.

Lemma 3.7. *Let G_s be the supergrid graph constructed from a planar bipartite graph B by Algorithm SupergridConstruction, and let $T = T(u, v; w)$ be a tentacle of G_s. If G_s has a Hamiltonian cycle HC, then there exists a Hamiltonian cycle HC^* in G_s such that $HC^*_{|T}$ is a Hamiltonian (s, t)-path of T for $s, t \in \{u, v, w\}$.*

Proof. By the construction of G_s, tentacle T satisfies the following properties:
(1) only three vertices u, v, w of T are adjacent to vertices of $G_s - T$, i.e., no vertex of $T - \{u, v, w\}$ is adjacent to vertices of $G_s - T$,
(2) each of twin corners u, v of T is adjacent to only two vertices p, q of $G_s - T$, i.e., $N(u) \cap (G_s - T) = N(v) \cap (G_s - T) = \{p, q\}$ and u, v, p, q forms a clique, and
(3) the tail corner w of T is adjacent to only one vertex r of $G_s - T$, i.e., $N(w) \cap (G_s - T) = \{r\}$.

Since only three vertices u, v, w of T are adjacent to vertices of $G_s - T$, $G_s - T$ and $T - \{u, v, w\}$ are disjoint. Then, the number of paths in $HC_{|T}$ is not larger than 2, i.e., $|HC_{|T}| \leqslant 2$. If $|HC_{|T}| = 1$, i.e., $HC_{|T}$ is either a return path or a cross path of T, then the lemma is clearly true. Assume that $|HC_{|T}| = 2$ below. Let $u_1, u_2, u_3 \in \{u, v, w\}$ and let $HC = P_1 \to u_1 \to Q_1 \to u_2 \to P_2 \to u_3 \to Q_2$, where $HC_{|T} = \{u_1 \to Q_1 \to u_2, u_3 \to Q_2\}$ and $P_2 \neq \emptyset$. Suppose that $P_1 = \emptyset$. Since HC is a Hamiltonian cycle of G_s, $u_1 \sim end(Q_2)$ and hence $HC_{|T} = \{u_2 \to \mathrm{rev}(Q_1) \to$

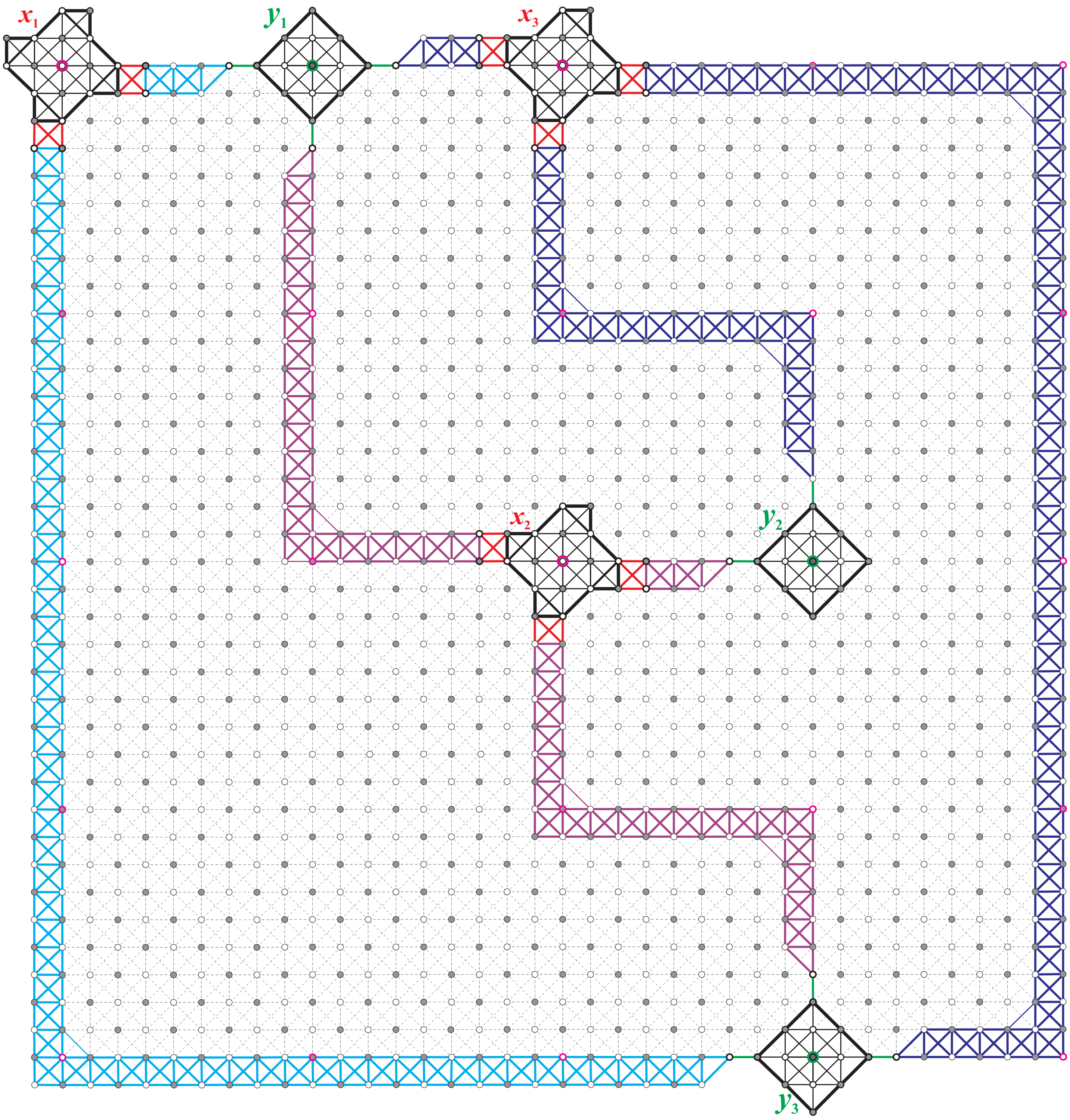

Fig. 14: A supergrid graph G_s constructed from a planar bipartite graph $B = (V_0 \cup V_1, E)$ with maximum degree 3 shown in Fig. 5(a), where solid lines indicate the edges in the constructed supergrid graph.

$u_1 \to \text{rev}(Q_2) \to u_3\}$, a contradiction. Thus, $P_1 \neq \emptyset$. On the other hand, suppose that $Q_2 \neq \emptyset$. Since HC is a cycle, $end(Q_2) \sim start(P_1)$ and hence there exist four vertices, $u_1, u_2, u_3, end(Q_2)$, of T which are adjacent to vertices of $G_s - T$, a contradiction. Thus, $Q_2 = \emptyset$. Then, $HC = P_1 \to u_1 \to Q_1 \to u_2 \to P_2 \to u_3$, where $P_1 \neq \emptyset$, $start(P_1) \sim u_3$, and $HC_{|T} = \{u_1 \to Q_1 \to u_2, u_3\}$. Since $u_3 \sim start(P_1)$ and $u_3 \sim end(P_2)$, $|N(u_3) \cap (G_s - T)| \geqslant 2$ and hence $u_3 \in \{u, v\}$. Then, $start(P_1), end(P_2) \in \{p, q\}$ and $start(P_1) \sim end(P_2)$. Let $P = P_2 \to P_1$. Then, $start(P)(= start(P_2)) \sim u_2$ and $end(P)(= end(P_1)) \sim u_1$. By Lemma 3.5, there exists a Hamiltonian (u_1, u_2)-path Q of T for $u_1, u_2 \in \{u, v, w\}$. Let $HC^* = P \to Q$. Then, HC^* is the desired Hamiltonian cycle of G_s such that $HC^*_{|T} = \{Q\}$ and Q is a Hamiltonian (s, t)-path of T for $s = u_1$ and $t = u_2$. In fact, Q is a cross path of T. Thus, the lemma holds true. □

By using the above lemma, we will prove the following lemma.

Lemma 3.8. *Let $B = (V_0 \cup V_1, E)$ be a planar bipartite graph with maximum degree 3 and let G_s be the supergrid graph constructed from B by Algorithm SupergridConstruction. Then, graph G_s has a Hamiltonian cycle if and only if there exists a Hamiltonian cycle in graph B.*

Proof. *If part*: In this part, we will prove that if graph B has a Hamiltonian cycle, then graph G_s contains a Hamiltonian cycle. Assume that the planar bipartite graph $B = (V_0 \cup V_1, E)$ has a Hamiltonian cycle HC_B. We will construct the corresponding Hamiltonian cycle HC of G_s as follows. Let (x, y) be an edge of graph B such that $x \in V_0$ and $y \in V_1$, and let the edge be simulated by a tentacle $T_{xy} = T(u, v; w)$ in G_s. Starting to form HC, we will cover T_{xy} by a cross path if $(x, y) \in HC_B$, and by a return path otherwise. By Lemma 3.5, there exists a cross path or return path of tentacle T_{xy}. The clusters themselves are covered as in Propositions 3.3 and 3.4. The partial paths can be connected to constitute a Hamiltonian cycle. Note that some critical edges of $e_i's$ for connecting to a return path in Fig. 7(a) must be deleted in the constructed Hamiltonian cycle. For example, for the planar bipartite graph $B = (V_0 \cup V_1, E)$ shown in Fig. 5(a), $HC_B = x_1 \to y_1 \to x_2 \to y_2 \to x_3 \to y_3$ is a Hamiltonian cycle of B. Then, Fig. 15 depicts its corresponding Hamiltonian cycle HC in the constructed supergrid graph G_s as shown in Fig. 14.

Only If part: In this part, we will prove that if graph G_s has a Hamiltonian cycle, then graph B contains a Hamiltonian cycle. Assume now that supergrid graph G_s has a Hamiltonian cycle HC. By Lemma 3.7, we may assume that for any tentacle $T = T(u, v; w)$ in G_s, the restriction $HC_{|T}$ of HC to T is a Hamiltonian (s, t)-path for $s, t \in \{u, v, w\}$. Then, by our construction of G_s each tentacle is covered by either a cross path or a return path. In our construction of G_s, each tentacle is connected to only one critical edge of a white cluster, and each white cluster is attached to at most three tentacles. On the other hand, each tentacle is connected to only one corner vertex of a black cluster, and each black cluster is connected to at most three tentacles. We can see that in HC each white or black cluster is incident upon exactly two cross paths. Note that each vertex of B is transformed into a cluster, and every edge of B is simulated by a tentacle. To construct a Hamiltonian cycle HC_B of graph B, we include in HC_B all edges corresponding to tentacles covered by cross paths. And each vertex of HC_B is a center of one cluster in G_s. Then, HC_B is a Hamiltonian cycle of graph B because each cluster (white or black) of G_s can not be covered by HC unless it is incident upon exactly two cross paths. □

Clearly, the Hamiltonian cycle problem for supergrid graphs is in NP. By Lemmas 3.6 and 3.8, we conclude the following theorem.

Theorem 3.9. *The Hamiltonian cycle problem for supergrid graphs is NP-complete.*

By similar arguments in proving the above theorem, we can prove the Hamiltonian path problem on supergrid graphs to be also NP-complete, as in the following theorem.

Theorem 3.10. *The Hamiltonian path problem for supergrid graphs is NP-complete.*

Proof. We give a reduction from the Hamiltonian cycle problem on planar bipartite graphs with maximum degree 3. Given a planar bipartite graph B with maximum degree 3, we construct a supergrid graph G'_s as follows:

1. construct a supergrid graph G_s by Algorithm SupergridConstruction;
2. let C_b be a black cluster of G_s such that its one critical edge (s', t') is not attached to any tentacle;
3. two new vertices s and t are added to be adjacent to s' and t', respectively, such that the degree of each new vertex is 1;

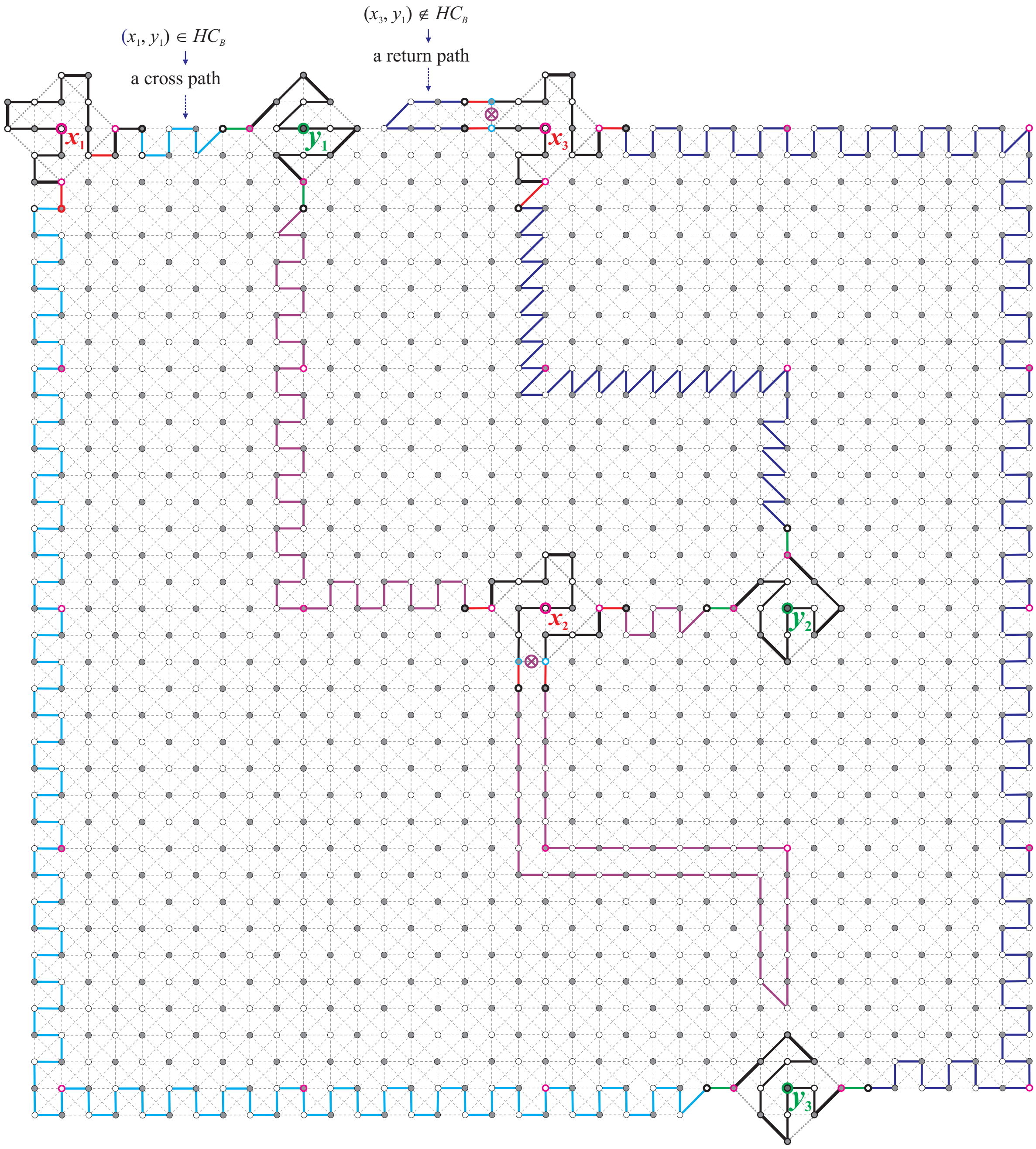

Fig. 15: A Hamiltonian cycle HC of a supergrid graph G_s constructed from a Hamiltonian cycle $HC_B = x_1 \rightarrow y_1 \rightarrow x_2 \rightarrow y_2 \rightarrow x_3 \rightarrow y_3$ of a planar bipartite graph B shown in Fig. 5(a), where solid lines indicate the edges in the cycle and ⊗ represents the destruction of an edge while constructing such a cycle.

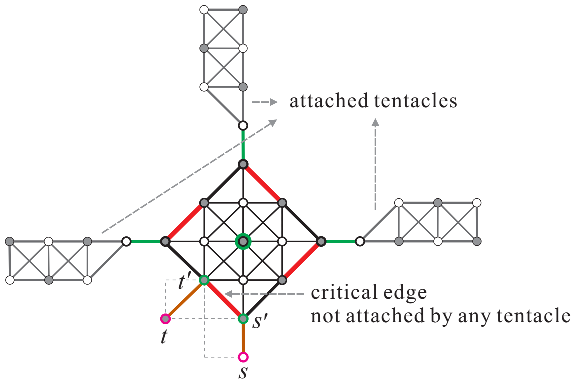

Fig. 16: A black cluster C_b in G'_s with two terminals s and t.

4. let the resultant supergrid graph be G'_s.

Since the degree of each vertex in B is at most 3, each tentacle is connected to one critical edges, and there are four critical edges in each black cluster, black cluster C_b of G_s does exist. The construction for attaching two new vertices is depicted in Fig. 16. By similar arguments in proving Lemma 3.8, we can verify that

graph G'_s has a Hamiltonian (s, t)-path if and only if there exists a Hamiltonian cycle in graph B.

Then, Lemma 3.8 and NP-completeness of the Hamiltonian cycle problem for planar bipartite graphs with maximum degree 3 complete the proof of this theorem. □

4. The Hamiltonian cycle problem on rectangular and alphabet supergrid graphs

In this section, we will study the Hamiltonian cycle property of rectangular and alphabet supergrid graphs. We show that these two subclasses of supergrid graphs always contain Hamiltonian cycles. In the literature, Chen *et al.* [6] and Salman [33] showed the Hamiltonian properties of rectangular and alphabet grid graphs, respectively, as shown in the following two lemmas.

Lemma 4.1. *(See [6].) Let $R'(m,n)$ with $m, n \geqslant 2$ be a rectangular grid graph which is a subgraph of $R(m,n)$, where $V(R'(m,n)) = \{v = (v_x, v_y) \mid 1 \leqslant v_x \leqslant m$ and $1 \leqslant v_y \leqslant n\}$. Then, $R'(m,n)$ contains a Hamiltonian cycle if and only if mn is even.*

Lemma 4.2. *(See [33].) Let $L'(m,n)$ with $m, n \geqslant 3$ be an L-aphabet grid graph which is a subgraph of $L(m,n)$, where $L'(m,n)$ is defined similar to $L(m,n)$. Then, $L'(m,n)$ has a Hamiltonian cycle if and only if mn is even.*

Since any rectangular grid graph $R'(m,n)$ is a subgraph of a rectangular supergrid graph $R(m,n)$, $R(m,n)$ contains a Hamiltonian cycle if mn is even. However, we will show that $R(m,n)$ contains a Hamiltonian cycle even if mn is odd. Obviously, 1-rectangle contains no Hamiltonian cycle. Without loss of generality, assume that $m \geqslant n$ for $R(m,n)$. For a 2-rectangle $R(m,2)$, we can construct a Hamiltonian cycle by visiting all boundary edges of $R(m,2)$. In the following, consider $R(m,n)$ to satisfy that $m \geqslant n \geqslant 3$. By definition, $R(m,n)$ consists of m columns and n rows of vertices. Let a_{ij} be the vertex locating at i-th row and j-th column of $R(m,n)$. That is, (i, j) is the coordinates of a_{ij} when a_{11} is coordinated as $(1,1)$. Let C be a cycle of $R(m,n)$ and let H be a boundary of $R(m,n)$, where H is a subgraph of $R(m,n)$. Recall that the restriction of C to H is denoted by $C_{|H}$. If $|C_{|H}| = 1$, i.e. $C_{|H}$ visits all boundary edges of H, then $C_{|H}$ is called *flat face* on H. If $|C_{|H}| > 1$ and $C_{|H}$ contains at least one boundary edge of H, then $C_{|H}$ is called *concave face* on H.

We first consider 3-rectangle $R(m,3)$. A Hamiltonian cycle of $R(m,3)$ is called *canonical* if it contains three flat faces on two shorter boundaries and one longer boundary, and it contains one concave face on the other boundary,

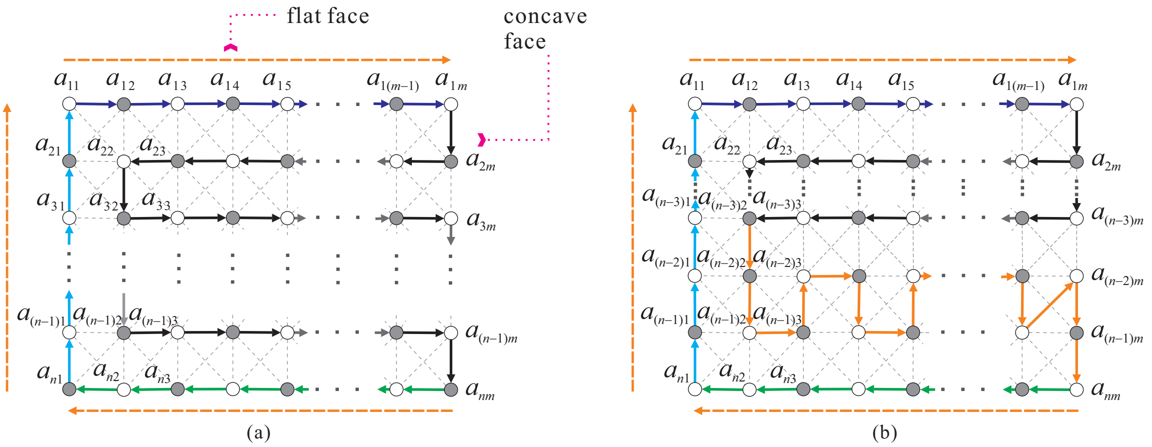

Fig. 17: The canonical Hamiltonian cycle of rectangular supergrid graph $R(m, n)$ for (a) n is even, and (b) n is odd, where $m \geqslant n \geqslant 4$, solid arrow lines indicate the edges in the cycle, and dashed arrow lines indicate the flat faces in the cycle.

where the shorter boundary contains three vertices. The following lemma shows that $R(m, 3)$ contains a canonical Hamiltonian cycle.

Lemma 4.3. *Let $R(m, 3)$ be a 3-rectangle with $m \geqslant 3$. Then, $R(m, 3)$ contains a canonical Hamiltonian cycle.*

Proof. We prove this lemma by constructing a Hamiltonian cycle of $R(m, 3)$ such that it contains all boundary edges of two shorter boundaries and one longer boundary, and it contains at least one boundary edge in the other longer boundary. By inspection, the lemma can be easily verified for $4 \geqslant m \geqslant 3$. In the following, assume that $m \geqslant 5$. Let $P_{\ell_1} = a_{11} \to a_{12} \to \cdots \to a_{1(m-1)} \to a_{1m}$, and let $P_\iota = a_{2\iota} \to a_{3\iota}$ for $m \geqslant \iota \geqslant 1$. Depending on whether m is even or not, we consider the following two cases:

Case 1: m is even. Let $P_{\ell_2} = \mathrm{rev}(P_2) \to P_3 \to \cdots \to \mathrm{rev}(P_j) \to P_{j+1} \to \cdots \to \mathrm{rev}(P_{m-2}) \to P_{m-1}$, where j is even and $2 \leqslant j \leqslant m-2$. Then, $P_{\ell_1} \to P_m \to \mathrm{rev}(P_{\ell_2}) \to \mathrm{rev}(P_1)$ is a canonical Hamiltonian cycle of $R(m, 3)$.

Case 2: m is odd. Let $P_{\ell_2} = \mathrm{rev}(P_2) \to P_3 \to \cdots \to \mathrm{rev}(P_j) \to P_{j+1} \to \cdots \to \mathrm{rev}(P_{m-3}) \to P_{m-2} \to \mathrm{rev}(P_{m-1})$, where j is even and $2 \leqslant j \leqslant m-3$. Then, $P_{\ell_1} \to P_m \to \mathrm{rev}(P_{\ell_2}) \to \mathrm{rev}(P_1)$ is a canonical Hamiltonian cycle of $R(m, 3)$.

It immediately follows from the above cases that the lemma holds true. □

We have constructed Hamiltonian cycles for 2-rectangles and 3-rectangles. In the following, let $R(m, n)$ satisfy $m \geqslant n \geqslant 4$. A Hamiltonian cycle of $R(m, n)$ with $m \geqslant n \geqslant 4$ is called *canonical* if it contains three flat faces on three boundaries, and it contains one concave face on the other boundary. The following lemma shows the Hamiltonian property of $R(m, n)$ with $m \geqslant n \geqslant 4$.

Lemma 4.4. *Let $R(m, n)$ be a rectangular supergrid graph with $m \geqslant n \geqslant 4$. Then, $R(m, n)$ contains four canonical Hamiltonian cycles with concave faces being on different boundaries.*

Proof. Depending on whether n is even or not, we consider the following two cases to construct a canonical Hamiltonian cycle of $R(m, n)$:

Case 1: n is even. Let $P_1 = a_{11} \to a_{12} \to \cdots \to a_{1m}$, $P_\iota = a_{\iota 2} \to a_{\iota 3} \to \cdots \to a_{\iota m}$ for $n \geqslant \iota \geqslant 2$, and let $P_{n+1} = a_{21} \to a_{31} \to \cdots \to a_{(n-1)1} \to a_{n1}$. Let $P^* = \mathrm{rev}(P_2) \to P_3 \to \mathrm{rev}(P_4) \to P_5 \to \cdots \to P_j \to \mathrm{rev}(P_{j+1}) \to \cdots \to \mathrm{rev}(P_{n-2}) \to P_{n-1}$, where j is even and $2 \leqslant j \leqslant n-2$. Let $C_{\mathrm{even}} = P_1 \to P^* \to \mathrm{rev}(P_n) \to \mathrm{rev}(P_{n+1})$. Then, C_{even} is a canonical Hamiltonian cycle of $R(m, n)$. The construction of such a canonical Hamiltonian cycle is depicted in Fig. 17(a).

Case 2: n is odd. In this case, $n \geqslant 5$. Let $P_1 = a_{11} \to a_{12} \to \cdots \to a_{1m}$, $P_\iota = a_{\iota 2} \to a_{\iota 3} \to \cdots \to a_{\iota m}$ for $n-3 \geqslant \iota \geqslant 2$, $P_n = a_{n2} \to a_{n3} \to \cdots \to a_{nm}$, and let $P_{n+1} = a_{21} \to a_{31} \to \cdots \to a_{(n-1)1} \to a_{n1}$. Let $P^* = \mathrm{rev}(P_2) \to P_3 \to \mathrm{rev}(P_4) \to P_5 \to \cdots \to \mathrm{rev}(P_j) \to P_{j+1} \to \cdots \to \mathrm{rev}(P_{n-5}) \to P_{n-4} \to \mathrm{rev}(P_{n-3})$, where j is

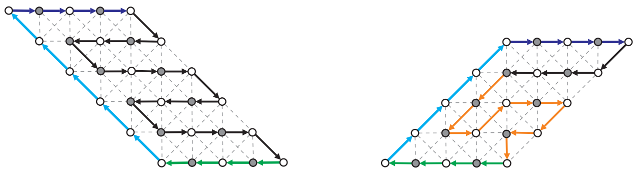

(a) (b)

Fig. 18: The Hamiltonian cycle for (a) parallelism supergrid graph $P(5,6)$, and (b) parallelism supergrid graph $P(5,5)$, where arrow lines indicate the edges in such cycles.

even and $2 \leqslant j \leqslant n-5$. If m is even, then let $P' = a_{(n-2)2} \to a_{(n-1)2} \to a_{(n-1)3} \to a_{(n-2)3} \to \cdots \to a_{(n-2)\tau_1} \to a_{(n-1)\tau_1} \to a_{(n-1)(\tau_1+1)} \to a_{(n-2)(\tau_1+1)} \to \cdots \to a_{(n-2)(m-2)} \to a_{(n-1)(m-2)} \to a_{(n-1)(m-1)} \to a_{(n-2)(m-1)} \to a_{(n-2)m} \to a_{(n-1)m}$; otherwise, let $P' = a_{(n-2)2} \to a_{(n-1)2} \to a_{(n-1)3} \to a_{(n-2)3} \to \cdots \to a_{(n-2)\tau_2} \to a_{(n-1)\tau_2} \to a_{(n-1)(\tau_2+1)} \to a_{(n-2)(\tau_2+1)} \to \cdots \to a_{(n-2)(m-3)} \to a_{(n-1)(m-3)} \to a_{(n-1)(m-2)} \to a_{(n-2)(m-2)} \to a_{(n-2)(m-1)} \to a_{(n-1)(m-1)} \to a_{(n-2)m} \to a_{(n-1)m}$, where τ_1, τ_2 are even, $2 \leqslant \tau_1 \leqslant m-2$, and $2 \leqslant \tau_2 \leqslant m-3$. Let $C_{\mathrm{odd}} = P_1 \to P^* \to P' \to \mathrm{rev}(P_n) \to \mathrm{rev}(P_{n+1})$. Then, C_{odd} is a canonical Hamiltonian cycle of $R(m,n)$. The construction of such a canonical Hamiltonian cycle is depicted in Fig. 17(b).

By the above cases, we construct a canonical Hamiltonian cycle of $R(m,n)$ such that its concave face is on the right boundary. By symmetry, we can construct a canonical Hamiltonian cycle of $R(m,n)$ such that its concave face is on the left boundary. Consider that m is even or not. By symmetry and the same constructions in Case 1 and Case 2, we can construct two canonical Hamiltonian cycles of $R(m,n)$ such that their concave faces are respectively placed at the upper and down boundaries. Thus there are four canonical Hamiltonian cycles of $R(m,n)$ such that their concave faces are on the different boundaries (left, right, upper, and down boundaries). This completes the proof of the lemma. □

By similar constructions in the proofs of Lemmas 4.3 and 4.4, we can construct a Hamiltonian cycle of a parallelism supergrid graph. For instance, Fig. 18 shows the Hamiltonian cycles of parallelism supergrid graphs $P(5,6)$ and $P(5,5)$.

Next, we will investigate the Hamiltonian cycle property of alphabet supergrid graphs. By Lemma 4.2, an L-alphabet grid graph $L'(m,n)$ has a Hamiltonian cycle only if mn is even. However, for an L-alphabet supergrid graph $L(m,n)$ we will show that it always contains a Hamiltonian cycle. Two distinct edges $e_1 = (u_1, v_1)$ and $e_2 = (u_2, v_2)$ of a graph G are called *parallel* if ($u_1 \sim v_1$ and $u_2 \sim v_2$) or ($u_1 \sim v_2$ and $u_2 \sim v_1$), denote this by $e_1 \approx e_2$. Let C_1 and C_2 be two vertex-disjoint cycles of a graph G. If there exist two edges $e_1 \in C_1$ and $e_2 \in C_2$ such that $e_1 \approx e_2$, then C_1 and C_2 can be combined into a cycle of G. Thus we have the following proposition.

Proposition 4.5. *Let C_1 and C_2 be two vertex-disjoint cycles in graph G. If there exist two edges $e_1 \in C_1$ and $e_2 \in C_2$ such that $e_1 \approx e_2$, then C_1 and C_2 can be combined into a cycle C.*

To construct a Hamiltonian cycle of an L-alphabet supergrid graph $L(m,n)$, we partition it into two adjacent rectangular supergrid subgraphs. Note that $L(m,n)$ is a subgraph of $R(3m-2, 5n-4)$ for $m, n \geqslant 3$. The L-alphabet supergrid graph $L(m,n)$ is separated into two disjoint rectangular supergrid subgraphs L_1 and L_2 such that $L_1 = R(m, 5n-4)$ and $L_2 = R(2m-2, n)$. The partition is depicted in Fig. 19(a). Since $m, n \geqslant 3$, we obtain that $5n-4 \geqslant 11$ and $2m-2 \geqslant 4$. By Lemmas 4.3 and 4.4, L_1 and L_2 contain canonical Hamiltonian cycles C_1 and C_2, respectively. We can place one flat face of C_1 to face the neighboring rectangular supergrid subgraph L_2 and place one flat face of C_2 to face L_1. Thus, there exist two parallel boundary edges $e_1 \in C_1$ and $e_2 \in C_2$. By Proposition 4.5, C_1 and C_2 can be combined into a Hamiltonian cycle of $L(m,n)$. For example, Fig. 19(b) shows a Hamiltonian cycle of $L(4,3)$. We then have the following lemma.

Lemma 4.6. *Let $L(m,n)$ be an L-alphabet supergrid graph with $m, n \geqslant 3$. Then, $L(m,n)$ contains a Hamiltonian cycle.*

By similar partition, we can separate the other types of alphabet supergrid graphs below.

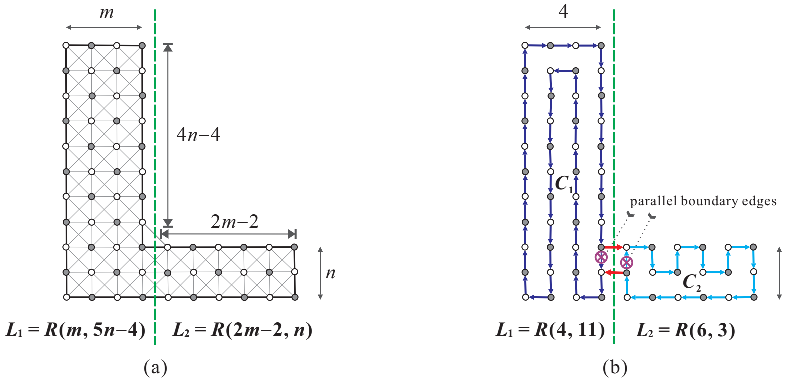

Fig. 19: (a) The partition of L-alphabet supergrid graph $L(m,n)$, where dashed line indicates the separation, and (b) a Hamiltonian cycle of $L(4,3)$, where arrow lines indicate the edges in the cycle and $\otimes$ represents the destruction of an edge while constructing such a Hamiltonian cycle.

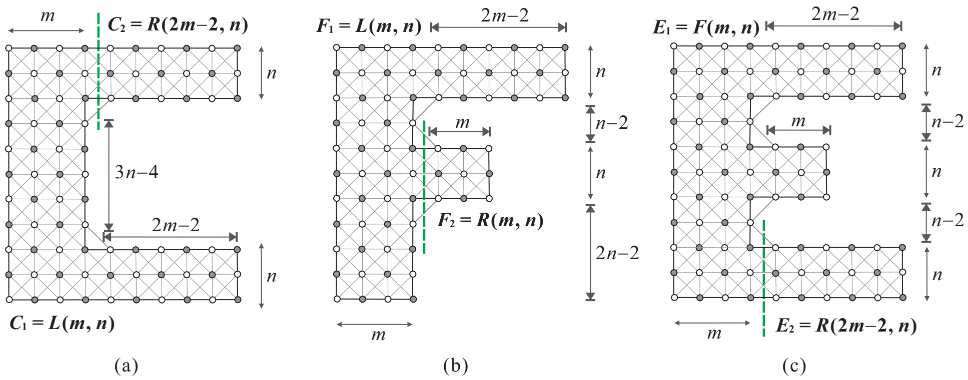

Fig. 20: The partitions of alphabet supergrid graphs for (a) C-alphabet, (b) F-alphabet, and (c) E-alphabet, where dashed lines indicate the separations.

Definition 4.1. The partitions of C-, F-, and E-alphabet supergrid graphs are defined as follows:
(1) A *partition* of an C-alphabet supergrid graph $C(m,n)$ is a separation of $C(m,n)$ into an L-alphabet supergrid subgraph $C_1 = L(m,n)$ and a rectangular supergrid subgraph $C_2 = R(2m-2,n)$.
(2) A *partition* of an F-alphabet supergrid graph $F(m,n)$ is a separation of $F(m,n)$ into an L-alphabet supergrid subgraph $F_1 = L(m,n)$ and a rectangular supergrid subgraph $F_2 = R(m,n)$.
(3) A *partition* of an E-alphabet supergrid graph $E(m,n)$ is a separation of $E(m,n)$ into an F-alphabet supergrid subgraph $E_1 = F(m,n)$ and a rectangular supergrid subgraph $E_2 = R(2m-2,n)$.

Fig. 20 depicts the partitions of the above alphabet supergrid graphs. By similar arguments in proving Lemma 4.6, the following lemma can be easily verified.

Lemma 4.7. *Let $C(m,n)$, $F(m,n)$, and $E(m,n)$ be an C-alphabet, an F-alphabet, and an E-alphabet supergrid graph, respectively, for $m,n \geqslant 3$. Then, $C(m,n)$, $F(m,n)$, and $E(m,n)$ contain Hamiltonian cycles.*

We have proved that rectangular, parallelism, and alphabet supergrid graphs are Hamiltonian. The following theorem concludes these results.

Theorem 4.8. *Let $A(m,n)$ be a rectangular or parallelism supergrid graph with $m,n \geqslant 2$, and let $B(m,n)$ be an L-alphabet, C-alphabet, F-alphabet, or E-alphabet supergrid graph with $m,n \geqslant 3$. Then, $A(m,n)$ and $B(m,n)$ contain Hamiltonian cycles.*

5. Concluding remarks

In this paper, we first proposed a novel class of graphs, namely supergrid graphs. The supergrid graphs contain grid graphs and triangular grid graphs as subgraphs. We also give an application to the Hamiltonian properties of supergrid graphs. Then, we prove that the Hamiltonian cycle and Hamiltonian path problems for supergrid graphs are NP-complete. Furthermore, we construct Hamiltonian cycles on some subclasses of supergrid graphs, including rectangular, parallelism, and alphabet supergrid graphs. It is interesting to see whether the Hamiltonian problems for the other subclasses of supergrid graphs, including solid and linear convex, are polynomial solvable. We would like to post it as an open problem to interested readers.

Acknowledgments

The authors gratefully acknowledge the helpful comments and suggestions of the reviewers, which have improved the presentation and have strengthened the contribution. This work is partly supported by the Ministry of Science and Technology of R.O.C. (Taiwan) under grant no. MOST 104-2221-E-324-003.

References

[1] N. Ascheuer, Hamiltonian path problems in the on-line optimization of flexible manufacturing systems, Technique Report TR 96-3, Konrad-Zuse-Zentrum für Informationstechnik, Berlin, 1996.
[2] J.C. Bermond, Hamiltonian graphs, in Selected Topics in Graph Theory ed. by L.W. Beinke and R.J. Wilson, Academic Press, New York, 1978.
[3] A.A. Bertossi, M.A. Bonuccelli, Hamiltonian circuits in interval graph generalizations, Inform. Process. Lett. 23 (1986) 195–200.
[4] J.A. Bondy, U.S.R. Murty, Graph Theory, 2nd Ed., Springer, New York, 2008.
[5] I. Bouchemakh, M. Zemir, On the broadcast independence number of grid graph, Graph. Combinator. 30 (2014) 83–100.
[6] S.D. Chen, H. Shen, R. Topor, An efficient algorithm for constructing Hamiltonian paths in meshes, Parallel Comput. 28 (2002) 1293–1305.
[7] C.W. Cheng, C.W. Lee, S.Y. Hsieh, Conditional edge-fault Hamiltonicity of Cartesian product graphs, IEEE Trans. Parallel Distribut. Syst. 24(10) (2013) 1951–1960.
[8] P. Damaschke, The Hamiltonian circuit problem for circle graphs is NP-complete, Inform. Process. Lett. 32 (1989) 1–2.
[9] M. Dettlaff, M. Lemańskaa, I.G. Yero, Bondage number of grid graphs, Discrete Appl. Math. 167 (2014) 94–99.
[10] M.R. Garey, D.S. Johnson, Computers and Intractability: A Guide to the Theory of NP-Completeness, Freeman, San Francisco, CA, 1979.
[11] M.C. Golumbic, Algorithmic Graph Theory and Perfect Graphs, Second edition, Annals of Discrete Mathematics 57, Elsevier, 2004.
[12] V.S. Gordon, Y.L. Orlovich, F. Werner, Hamiltonian properties of triangular grid graphs, Discrete Math. 308 (2008) 6166–6188.
[13] S. Gravier, Total domination number of grid graphs, Discrete Appl. Math. 121 (2002) 119–128.
[14] V. Grebinski, G. Kucherov, Reconstructing a Hamiltonian cycle by querying the graph: Application to DNA physical mapping, Discrete Appl. Math. 88 (1998) 147–165.
[15] S.Y. Hsieh, Y.R. Cian, Conditional edge-fault Hamiltonicity of augmented cubes, Inform. Sci. 180(13) (2010) 2596–2617.
[16] S.Y. Hsieh, C.Y. Wu, Edge-fault-tolerant hamiltonicity of locally twisted cubes under conditional edge faults, J. Comb. Optim. 19(1) (2010) 16–30.
[17] F.T. Hu, Y. Lu, J.M. Xu, The total bondage number of grid graphs, Discrete Appl. Math. 160 (2012) 2408–2418.
[18] K. Islam, H. Meijer, Y. Núñez, D. Rappaport, H. Xiao, Hamiltonian cycles in hexagonal grid graphs, in: Proceedings of the 19th Canadian Conference on Computational Geometry, CCCG'97, 2007, pp. 85–88.
[19] A. Itai, C.H. Papadimitriou, J.L. Szwarcfiter, Hamiltonian paths in grid graphs, SIAM J. Comput. 11(4) (1982) 676–686.
[20] D.S. Johnson, The NP-complete column: an ongoing guide, J. Algorithms 6 (1985) 434–451.
[21] F. Keshavarz-Kohjerdi, A. Bagheri, Hamiltonian paths in some classes of grid graphs, J. Appl. Math. 2012 (1982) article no. 475087.
[22] F. Keshavarz-Kohjerdi, A. Bagheri, A. Asgharian-Sardroud, A linear-time algorithm for the longest path problem in rectangular grid graphs, Discrete Appl. Math. 160 (2012) 210–217.
[23] M.S. Krishnamoorthy, An NP-hard problem in bipartite graphs, SIGACT News 7 (1976) 26.
[24] C.W. Lee, T.J. Lin, S.Y. Hsieh, Hamiltonicity of product networks with faulty elements, IEEE Trans. Parallel Distribut. Syst. 25(9) (2014) 2318–2331.
[25] W. Lenhart, C. Umans, Hamiltonian cycles in solid grid graphs, in: Proceedings of the 38th Annual Symposium on Foundations of Computer Science (FOCS'97), 1997, pp. 496–505.
[26] F. Luccio, C. Mugnia, Hamiltonian paths on a rectangular chessboard, in: Proceedings of the 16th Annual Allerton Conference, 1978, pp. 161–173.
[27] D. Marx, Eulerian disjoint paths problem in grid graphs is NP-complete, Discrete Appl. Math. 143 (2004) 336–341.
[28] B. Menke, T. Zamfirescu, C. Zamfirescu, Intersections of longest cycles in grid graphs, J. Graph Theory 25 (1997) 37–52.
[29] S. Muthammai, P. Vidhya, Total complementary tree domination in grid graphs, Intern. J. Math. Soft Comput. 3 (2013) 107–114.
[30] J.F. O'Callaghan, Computing the perceptual boundaries of dot patterns, Comput. Graphics Image Process. 3 (1974) 141–162.
[31] F.P. Preperata, M.I. Shamos, Computational Geometry: An Introduction, Springer, New York, 1985.
[32] J.R. Reay, T. Zamfirescu, Hamiltonian cycles in T-graphs, Discrete Comput. Geom. 24 (2000) 497–502.
[33] A.N.M. Salman, Contributions to Graph Theory, Ph.D. thesis, University of Twente, 2005.

[34] G.T. Toussaint, Pattern recognition and geometrical complexity, in: Proceedings of the 5th International Conference on Pattern Recognition, Miami Beach, 1980, pp. 1324–1347.
[35] C. Zamfirescu, T. Zamfirescu, Hamiltonian properties of grid graphs, SIAM J. Disc. Math. 5(4) (1992) 564–570.
[36] W.Q. Zhang, Y.J. Liu, Approximating the longest paths in grid graphs, Theoret. Comput. Sci. 412 (2011) 5340–5350.